

8-23-2011

Observations of hydroxyl and peroxy radicals and the impact of BrO at Summit, Greenland in 2007 and 2008

J Liao

Georgia Institute of Technology - Main Campus

L Gregory Huey

Georgia Institute of Technology - Main Campus

D Tanner

Georgia Institute of Technology - Main Campus

N Brough

British Antarctic Survey

Steve Brooks

NOAA

See next page for additional authors

Follow this and additional works at: https://scholars.unh.edu/earthsci_facpub

 Part of the [Atmospheric Sciences Commons](#)

Recommended Citation

Liao, J., Huey, L. G., Tanner, D. J., Brough, N., Brooks, S., Dibb, J. E., Stutz, J., Thomas, J. L., Lefer, B., Haman, C., and Gorham, K.: Observations of hydroxyl and peroxy radicals and the impact of BrO at Summit, Greenland in 2007 and 2008, *Atmos. Chem. Phys.*, 11, 8577-8591, doi:10.5194/acp-11-8577-2011, 2011.

This Article is brought to you for free and open access by the Earth Sciences at University of New Hampshire Scholars' Repository. It has been accepted for inclusion in Earth Sciences Scholarship by an authorized administrator of University of New Hampshire Scholars' Repository. For more information, please contact nicole.hentz@unh.edu.

Authors

J Liao, L Gregory Huey, D Tanner, N Brough, Steve Brooks, Jack E. Dibb, J Stutz, J L. Thomas, Barry Lefer, C Haman, and K Gorham

Observations of hydroxyl and peroxy radicals and the impact of BrO at Summit, Greenland in 2007 and 2008

J. Liao¹, L. G. Huey¹, D. J. Tanner¹, N. Brough², S. Brooks³, J. E. Dibb⁴, J. Stutz⁵, J. L. Thomas^{5,*}, B. Lefer⁶, C. Haman⁶, and K. Gorham⁷

¹School of Earth and Atmospheric Sciences, Georgia Institute of Technology, Atlanta, Georgia, USA

²British Antarctic Survey, Natural Environment Research Council, Cambridge, UK

³NOAA Atmospheric Turbulence and Diffusion Division, TN, USA

⁴Climate Change Research Center, Institute for the Study of Earth, Oceans and Space, University of New Hampshire, Durham, NH, USA

⁵University of California Los Angeles, Department of Atmosphere Ocean Science, Los Angeles, CA, USA

⁶Department of Geosciences, University of Houston, TX, USA

⁷Chemistry, University of California, Irvine, California, USA

* now at: UPMC Univ. Paris 06; Université Versailles St-Quentin; CNRS/INSU, UMR8190; LATMOS-IPSL, Paris, France

Received: 6 April 2011 – Published in Atmos. Chem. Phys. Discuss.: 26 April 2011

Revised: 4 August 2011 – Accepted: 7 August 2011 – Published: 23 August 2011

Abstract. The Greenland Summit Halogen-HO_x (GSHOX) Campaign was performed in spring 2007 and summer 2008 to investigate the impact of halogens on HO_x (=OH+HO₂) cycling above the Greenland Ice Sheet. Chemical species including hydroxyl and peroxy radicals (OH and HO₂+RO₂), ozone (O₃), nitrogen oxide (NO), nitric acid (HNO₃), nitrous acid (HONO), reactive gaseous mercury (RGM), and bromine oxide (BrO) were measured during the campaign. The median mid-day values of HO₂+RO₂ and OH concentrations observed by chemical ionization mass spectrometry (CIMS) were 2.7×10^8 molec cm⁻³ and 3.0×10^6 molec cm⁻³ in spring 2007, and 4.2×10^8 molec cm⁻³ and 4.1×10^6 molec cm⁻³ in summer 2008. A basic photochemical 0-D box model highly constrained by observations of H₂O, O₃, CO, CH₄, NO, and J values predicted HO₂+RO₂ ($R=0.90$, slope=0.87 in 2007; $R=0.79$, slope=0.96 in 2008) reasonably well and under predicted OH ($R=0.83$, slope=0.72 in 2007; $R=0.76$, slope=0.54 in 2008). Constraining the model to HONO observations did not significantly improve the ratio of OH to HO₂+RO₂ and the correlation between predictions and observations. Including bromine chemistry in the model constrained by observations of BrO improved the correlation between observed and predicted HO₂+RO₂ and OH, and brought the average hourly OH and HO₂+RO₂

predictions closer to the observations. These model comparisons confirmed our understanding of the dominant HO_x sources and sinks in this environment and indicated that BrO impacted the OH levels at Summit. Although, significant discrepancies between observed and predicted OH could not be explained by the measured BrO. Finally, observations of enhanced RGM were found to be coincident with under prediction of OH.

1 Introduction

Summit, Greenland (72°34'N, 38°29'W, alt=3.3 km) is located in the middle of the Greenland Ice Sheet and has been the site of a series of scientific studies beginning with ice coring in the 1980s (e.g. Hammer et al., 1980; Mayewski and Bender, 1995). In more recent years, the interaction between photochemically active species in the snowpack and the overlying atmosphere has been studied in detail at Summit and other polar stations (e.g. Dibb and Jaffrezo, 1997; Grannas et al., 2007; Jones et al., 2008; Davis et al., 2001; Huey et al., 2004). Elevated levels of species emitted from surface snow such as nitric oxide (NO), formaldehyde (CH₂O), and hydrogen peroxide (H₂O₂) have been observed over sunlit snow in a series of campaigns (Dibb et al., 2002, 2004; Honrath et al., 1999, 2002; Hutterli et al., 1999, 2001, 2004; Davis et al., 2001; Slusher et al., 2002; Helmig et al., 2008). Snowpack emissions of radical precursors (nitrous acid (HONO),



Correspondence to: L. G. Huey
(greg.huey@eas.gatech.edu)

H₂O₂, and CH₂O) and NO_x (NO + NO₂) have the potential to significantly enhance HO_x (hydroxyl (OH) + hydroperoxyl (HO₂) radicals) photochemistry in these locations (e.g. Yang et al., 2002; Chen et al., 2001).

The OH and peroxy radicals (HO₂ + RO₂) have been measured in a few polar locations and the concentrations vary based on the radical sources as well as environmental conditions. The daytime mean value of OH observed at Palmer station (64°46'S, 64°3.0'W) in Antarctica was 3×10^5 molec cm⁻³ in austral summer (Jefferson et al., 1998). The low OH levels were found to be consistent with the high solar zenith angle, extensive cloud coverage, no snow coverage, and low NO_x levels (typically near detection limits of 2–4 pptv) (Jefferson et al., 1998). OH concentrations observed at South Pole were unexpectedly high, with an average value of $2.0 (\pm 0.9) \times 10^6$ molecule cm⁻³ in November and December from three field campaigns ISCAT 98, ISCAT 00 and ANTICI 03 (Mauldin et al., 2001, 2004, 2010; Grannas et al., 2007). The high OH levels at South Pole were due to low boundary layer height and snowpack emissions that gave high levels of NO_x and to a lesser extent formaldehyde (Davis et al., 2001; Hutterli et al., 2004). A photochemical model constrained to CH₂O and H₂O₂ measurements predicted OH levels with a median modeled to observed (M/O) ratio of 1.27 (Chen et al., 2004). However, the M/O ratio for OH was found to vary with NO levels at South Pole (Chen et al., 2001, 2004). The model over predicted OH significantly at low NO (NO < 50 pptv; M/O > 1.5) and high NO (NO > 150 pptv; M/O = 1.5) levels but agreed better at moderate levels of NO (Chen et al., 2004). Sjostedt et al. (2007) measured OH (mean 6.3×10^6 molec cm⁻³) and HO₂ + RO₂ (mean 2.8×10^8 molec cm⁻³) levels at Summit, Greenland during summer 2003. The observed HO₂ + RO₂ levels agreed well with the model predictions, although the measured OH levels were elevated compared to the predictions (Sjostedt et al., 2007; Chen et al., 2007). Sjostedt et al. (2007) suggested that halogen may be present at Summit, perturbing the HO_x cycling and enhancing OH levels. In contrast, a later study at Halley Bay, Antarctica (75°35'S, 26°19'W) found average OH levels of 3.9×10^5 molec cm⁻³ in February with typical maximum (local noontime) levels of 7.9×10^5 molec cm⁻³ (Bloss et al., 2007, 2010). The OH levels at Halley Bay were slightly higher than measured at Palmer station in the same season of the year but significantly lower than observed at South Pole. The low levels of OH were surprising as mean diurnal NO levels of up to ~14 pptv and significant iodide oxide (IO) and bromine oxide (BrO) levels of up to ~7 pptv and ~9 pptv were observed. A photochemical box model including halogen reactions significantly over predicted observed levels of OH and HO₂, although the model well predicted the mean levels and diurnal patterns of NO_x (NO and NO₂) (Bloss et al., 2007, 2010). The mean daily maximum M/O ratio of OH was 3.8 and of HO₂ was 2.8. The mean observed HO₂ to OH ratio of 46 was in good agreement with the mean predicted value of 44 from

the model considering bromine and iodine chemistry, and no elevated OH was observed.

Prior to the GSHOX campaign, there was only indirect evidence that BrO may exist at Summit, Greenland. Although the overall reservoir of bromine at Summit is much less than in the coastal Arctic where ozone depletion events (ODEs) are typically observed, vertical profiles of ozone obtained from balloon borne sensors have demonstrated that ozone in the boundary layer is consistently depleted relative to the air above (Helmig et al., 2002). However, the reaction of NO (~20 pptv) and RO₂ (~10⁸ molec cm⁻³) in the boundary layer at Summit should give a local ozone production of ~2 ppbv day⁻¹ (Sjostedt et al., 2007). This type of ozone production is evident in the NO_x (NO + NO₂) rich South Pole boundary layer (Crawford et al., 2001) where boundary layer ozone is elevated relative to the air above (Helmig et al., 2002). In addition, mercury oxidation in snow has been observed at Summit, Greenland (Faïn et al., 2008; Brooks et al., 2011). As Br + Hg⁰ (GEM) → Hg²⁺ (RGM) is the only well established reaction that can initiate such rapid conversion of gaseous element mercury (GEM) to reactive gaseous mercury (RGM) (Ariya et al., 2002; Donohoue et al., 2006), depleted GEM and elevated RGM may be a signature of active bromine chemistry as RGM is a relatively short lived species (Steffen et al., 2008).

High levels (up to 30–40 pptv) of BrO are typically found in the polar marine boundary layer near large sources of halides during ODEs (Tuckermann et al., 1997; Hausmann and Platt, 1994; Saiz-lopez et al., 2007; Liao et al., 2011a). However, significant levels of BrO have been observed in a variety of other marine locations. For example, BrO was observed in the tropical marine boundary layer within the Cape Verde archipelago by Read et al. (2008) with an average daytime level of 2.5 pptv. Up to ~7 pptv of BrO was observed in the mid-latitude marine boundary at Roscoff, France (48.7° N, 4.0° W) (Mahajan et al., 2009) and at the Mace Head Atmospheric Research Station, Ireland (53.33° N, 9.90° W) (Saiz-lopez et al., 2006).

To investigate the hypothesis that BrO is present at Summit and that it impacts HO_x photochemistry, a suite of instruments were used to measure OH, HO₂ + RO₂, BrO and other species at Summit, Greenland in spring 2007 and summer 2008. The observations of OH and HO₂ + RO₂, and their comparison to photochemical models are presented in this paper. The BrO observations and the associated snowpack chemistry are discussed by Stutz et al. (2011) and Thomas et al. (2011), respectively.

2 Methods

A comprehensive collection of instruments were used at Summit, Greenland during May–June 2007 and June–July 2008 to measure trace gases and radicals, aerosols, actinic fluxes, and meteorological parameters. Table 1 provides a

Table 1. Summary of the measurements at Summit, Greenland 2007–2008.

Species and parameters	Instrument	Uncertainty	Institution	Reference
O ₃	UV absorption ozone analyzer	< ±5 %	Ga. Tech	
NO	Chemilluminant gas analyzer	±10 %	Ga. Tech	Ryerson et al. (2000)
CO	Canister/GC	< ±5 %	UCI	Swanson et al. (2002)
CH ₄	Canister/GC	< ±5 %	UCI	Swanson et al. (2002)
NMHC	Canister/GC	< ±5 %	UCI	Swanson et al. (2002)
OH	CIMS	±30 %	Ga. Tech	Sjostedt et al. (2007)
HO ₂ + RO ₂	CIMS	±35 %	Ga. Tech	Sjostedt et al. (2007)
BrO	CIMS	±30 % –36 %	Ga. Tech	Liao et al. (2011a)
BrO	DOAS	±10 %	UCLA	Stutz et al. (2011)
SMPS _N	SMPS/CPC	±10 %	UNH	Ziemba et al. (2010)
SMPS _S	SMPS/CPC	±10 %	UNH	Ziemba et al. (2010)
GEM	Tekran	±2 %	NOAA	Brooks et al. (2011)
RGM	Tekran	±5 %	NOAA	Brooks et al. (2011)
FPM	Tekran	±5 %	NOAA	Brooks et al. (2011)
HNO ₃	Mist Chamber	±15 % –20 %	UNH	Dibb et al. (1998)
Soluble Bromine	Mist Chamber	±15 % –20 %	UNH	Dibb et al. (1998)
HONO	Mist Chamber	±15 % –20 %	UNH	Dibb et al. (1998)
Actinic Flux	SAFS	±10 %	U. Houston	Shetter and Müller (1999)
Temperature	F-Thermocouples	±0.5 °C	U. Houston	Haman et al. (2011)
WS/WD	AWS/Digital compass		U. Houston	Haman et al. (2011)

summary of the measurements during the campaign. The details of measurement techniques not specifically summarized are presented in the references in Table 1. Most of the measurements were located in a satellite camp ~1 km to the south of the main station. The layout of the experiment is shown in Fig. 1.

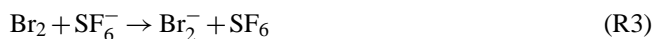
2.1 HO_x measurement by CIMS

The chemical ionization mass spectrometry (CIMS) instrument to measure HO_x (OH and sum of HO₂ + RO₂) is nearly identical to that used to measure HO_x in 2003 (Sjostedt, 2006 and Sjostedt et al., 2007). The basic methods are based on the work of Tanner et al. (1997). The CIMS was calibrated for OH and HO₂. Because many of the simple RO₂ species (e.g. CH₃O₂) are efficiently converted to HO₂ by this method (Edwards et al., 2003), we assumed that the sensitivities for RO₂ were the same as for HO₂. The CIMS was located in the satellite camp (Fig. 1) and the inlet was about 1.5 m above the snow surface. The dominant uncertainty in the OH and HO₂ + RO₂ measurements is the accuracy of the calibration source (Sjostedt et al., 2007). The combined uncertainties are estimated to be ~30 % for OH measurements and ~35 % for HO₂ + RO₂ measurements. The calibration standards for both OH and HO₂ measurements are produced from the photolysis of ambient water vapor, consequently, the uncertainty in the ratio of observed OH to HO₂ + RO₂ is smaller than the absolute uncertainties.

2.2 BrO measurement by CIMS

The CIMS used to measure BrO levels at Summit is essentially identical to the low pressure CIMS systems used to measure halogens on the NASA DC-8 and NOAA P3 aircrafts during the ARCTAS and ARCPAC campaigns (Neuman et al., 2010), and at Barrow, Alaska during the OASIS 2009 campaign (Liao et al., 2011a). The details of the instrument and air sampling inlet are described in (Liao et al., 2011a) and only significant differences are described here.

SF₆[−] was used as a reagent ion to ionize BrO and other species such as SO₂.



The charge transfer reaction of SF₆[−] with BrO (Reaction R2) was observed for the first time as part of this work. The rate constant for this reaction was determined relative to that of SF₆[−] with Br₂ (Reaction R3) (Streit, 1982). BrO was synthesized from the reaction of O(³P) with Br₂ in excess ozone as described in Liao et al. (2011a). The ratio of the rate constant for Reaction (R3) to Reaction (R2) was determined to be 1.0 ± 25 % in the laboratory. The rate constant for Reaction (R2) derived from this work is (5 ± 2) × 10^{−10} molec cm^{−3} s^{−1}.

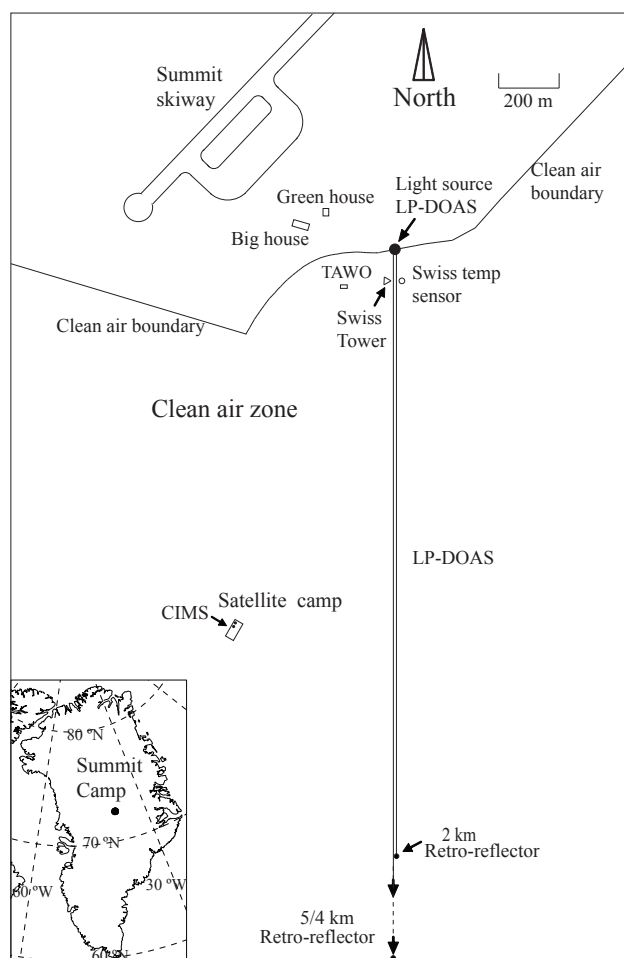


Fig. 1. The layout of the CIMS and LP-DOAS instruments in the Summit campaign.

SO₂ was used as our primary calibration gas for determining the sensitivity of the CIMS system in the field (Kim et al., 2007; Slusher et al., 2001) and as a proxy to track the sensitivity of BrO. The ratio of the sensitivity of BrO to that of SO₂ was determined in the laboratory after the campaign as a function of dew point (dewpt). The average sensitivity of SO₂ was $\sim 4 \text{ Hz pptv}^{-1}$ in 2007 and $\sim 60 \text{ Hz pptv}^{-1}$ in 2008 summit campaign. The sensitivity ratio of SO₂ to BrO was determined as Eq. (1)

$$\frac{\text{SO}_2}{\text{BrO}} = \begin{cases} 0.76 - 0.096 \times \text{dewpt} - 0.00154 \times \text{dewpt} & (\text{dewpt} > -35^\circ\text{C}) \\ 2.2 & (\text{dewpt} < -35^\circ\text{C}). \end{cases} \quad (1)$$

The background signal level of BrO during the 2007 Summit campaign was determined by periodically scrubbing the sampled air with an active carbon filter, similar to that used before for removal of SO₂, HO₂NO₂, and HNO₃. In 2008 the background was determined by using glass wool because it was found to effectively remove halogen species (Neuman et al., 2010).

The detection limits of BrO measurements are estimated to be $\sim 1.8 \text{ pptv}$ in 2007 and $\sim 0.7 \text{ pptv}$ in 2008. Considering the uncertainty in SO₂ standard concentration ($\sim 10\%$), the uncertainties in the sensitivity ratios between BrO and Br₂ ($\sim 25\%$) and between Br₂ and SO₂ ($\sim 5\%$), the total uncertainty in BrO measurements is estimated to be $\sim 36\%$. The concentrations of BrO at Summit in spring 2007 and summer 2008 were often near the detection limits of both instruments (detection limit of LP DOAS = $0.5\text{--}2 \text{ pptv}$; detection limit of CIMS = $\sim 1\text{--}2 \text{ pptv}$). Moreover, the measurements of BrO at Summit were the earliest applications of CIMS to measure ambient BrO. SF₆[−] was used as the reagent ion to detect BrO at that time. After these campaigns the more selective reagent ion, I[−], was found to sensitively detect BrO (Neuman et al., 2010). In addition, the capability of CIMS, using I[−], to accurately and sensitively measure BrO was demonstrated in Liao et al. (2011a). Moving forward, CIMS observations of BrO with I[−] are preferred to SF₆[−] as the latter ion is more prone to interferences as it is more reactive (Huey et al., 1995). Consequently, conclusions drawn from the CIMS BrO observations in this study must be considered in the context of potential interferences, although the specific candidates for the interference are not known at this time.

2.3 BrO measurement by DOAS

The primary BrO measurement during the Summit campaign was a long path differential absorption spectrometer (LP DOAS). The techniques of the LP DOAS instrument were based on the work of Stutz and Platt (1997). The LP DOAS measured BrO over a path of either 2 km or 5 km (2007)/4 km (2008). The optical paths were 1.5–3 m above the snow. The LP DOAS telescope was located at the edge of the clean air boundary in the south of the station and two reflectors were located 2 km and 5 km (2007)/4 km (2008) to the South of the light source (Fig. 1). The details of BrO measurement by LP DOAS are provided by Stutz et al. (2011).

2.4 Mercury measurement

Tekran models 2537a/1130/1135 (Brooks et al., 2008) were used to measure gaseous elemental mercury (GEM), reactive gaseous mercury (RGM), also known as gaseous oxidized mercury (GOM), and fine particle mercury (FPM) via cold vapor atomic fluorescence. The details of the mercury measurements are described in the work of Brooks et al. (2011).

2.5 Actinic Fluxes measurement

Actinic Fluxes were measured by a Scanning Actinic Flux Spectrometer (SAFS) (Shetter and Muller, 1999) by University of Houston. The photolysis rate coefficients (*J* values) of atmospheric compounds were calculated based on the sum of downwelling and upwelling Actinic Fluxes.

2.6 Photochemical models

A 0-Dimensional steady-state $\text{HO}_x\text{-NO}_x\text{-CH}_4$ model is used to evaluate the HO_x chemistry at Summit. The model is identical to that described in Sjostedt et al. (2007) and is denoted as the base model (BM). The BM involves 46 chemical reactions which include 8 photolysis reactions and is constrained by the measurements of photolysis rate coefficients (J values) and the following gases: H_2O , O_3 , CO , CH_4 , and NO . The model only considered CH_4 chemistry because previous studies by Chen et al. (2007) and Sjostedt et al. (2007) found that including nonmethane hydrocarbons (NMHC) decreased OH number densities and increased $\text{HO}_2 + \text{RO}_2$ number densities less than 10 % and that most of the RO_2 is CH_3O_2 at Summit, Greenland. Typical levels of the dominant NMHC species ethane, propane, and butane are 1.0 ppbv, 0.07 ppbv, and 0.04 ppbv, respectively. The NMHC measured in 2007 and 2008 were generally consistent with the measurements in 2003. The average ethane, propane and butane levels were 1.1 ppbv, 0.14 ppbv, 0.03 ppbv, respectively in spring 2007 and 0.9 ppbv, 0.07 ppbv, 0.02 ppbv respectively in summer 2008. Because Summit Greenland is in the middle of Greenland Ice Sheet far away from biogenic and anthropogenic volatile organic carbons (VOCs) sources, we do not expect high levels of oxygenated VOCs reacting with OH at Summit, Greenland. Measurements of larger oxygenated VOCs at Summit, Greenland are needed to validate our assumption. The input data used to constrain the model were averaged to a 10 min basis. A spin-up time of 1000 s was used for model calculations of relatively long-lived species (e.g. H_2O_2 and HCHO). The model predictions are compared to OH and $\text{HO}_2 + \text{RO}_2$ measurements (assuming RO_2 is primarily CH_3O_2). The rate constants are taken from the JPL compilation (Sander et al., 2006), and the J values are derived from the measured actinic fluxes (Shetter and Muller, 1999). Similar to the work of Sjostedt et al. (2007), the model can be run either constrained or unconstrained to HONO measurements. This allows evaluation of the impact of HONO on HO_x levels and the radical budget. The model constrained to HONO observations is referred as BM.HONO.

To examine the impact of BrO on HO_x levels, bromine reactions (see Table 2) were added to the BM. The model incorporating the bromine chemistry is referred as BM.BrO. Reaction (R6) (in Table 2) acts as a source of HO_x . HOBr serves as a temporary reservoir of HO_x and heterogeneous loss of HOBr is effectively a loss of HO_x . HOBr levels were assumed to be in steady-state and controlled by Reactions (R2), (R8) and (R9) (in Table 2). This assumption was valid because the photolysis lifetime of HOBr is relatively short (~ 5 min) at Summit Greenland in the daytime. The assumption was also found to reasonably predict the observed HOBr in Liao et al. (2011b). The box model is constrained by BrO measurements from CIMS and LP DOAS to illustrate the effect of two BrO datasets on HO_x levels. The mass accommodation coefficient of HOBr is assumed

to be 0.6 (Wachsmuth et al., 2002). This allowed predictions of OH and $\text{HO}_2 + \text{RO}_2$ when BrO measurements were available. The model did not include the heterogeneous sinks of BrONO_2 because the model is constrained to BrO measurements and BrONO_2 does not directly impact the budget of OH and $\text{HO}_2 + \text{RO}_2$. The impact of BrONO_2 on daytime NO_2 levels is also small due to the low BrO concentrations. Daytime NO_2 levels increased ~ 5 % in 2007 and ~ 2 % in 2008 when the model considered bromine Reactions (R4) and (R5) in the Table 2. As the photochemical lifetime (~ 2 min) of HO_2 is much shorter than the lifetime due to heterogeneous loss (~ 150 min) with a uptake coefficient of 0.1 (Mao et al., 2010), the model did not consider the heterogeneous loss of HO_2 .

One significant difference from the work of Sjostedt et al. (2007) is that observations of CH_2O and H_2O_2 were not available. For this reason, the BM was used to predict CH_2O and H_2O_2 levels. In order to test the ability of the model to calculate these species, predictions of CH_2O and H_2O_2 using data from the 2004 Summit campaign were compared to observations. Both CH_2O and H_2O_2 predictions are in reasonable agreement with the measurements (CH_2O : $R = 0.68$, mean $\text{M/O} = 1.3$; H_2O_2 : $R = 0.72$, mean $\text{M/O} = 2.4$), which suggests that the steady state model is viable for estimation of CH_2O and H_2O_2 within about a factor of two. The impact of this relatively high uncertainty in mixing ratios of CH_2O and H_2O_2 on predictions of HO_x and its partitioning are discussed in Sect. 4.2.

3 Results

3.1 OH and ($\text{HO}_2 + \text{RO}_2$) observations

The time series of observations of OH, $\text{HO}_2 + \text{RO}_2$, $J(\text{O}^1\text{D})$, BrO, NO, HNO_3 , HONO, O_3 , RGM, temperature, wind speeds and wind directions on a 10 min time base in spring 2007 and summer 2008 are shown in Fig. 2. The observations of OH and $\text{HO}_2 + \text{RO}_2$ were filtered to exclude the periods when $\text{NO} > 50$ pptv. High NO mixing ratios at Summit are almost always due to pollution plumes from the station power generator. High NO dramatically brought down the $\text{HO}_2 + \text{RO}_2$ concentrations and raised the OH concentrations (Fig. 3). Similar phenomena were observed by previous works as well (e.g. Sjostedt et al., 2007; Bloss et al., 2007). The HO_x instrument was shut down to save reagent gases at night (22:00–06:00 Western Greenland Standard Time (WGST)) when the OH concentrations decreased to near detection limit ($10^5 \text{ molec cm}^{-3}$). The gaps in the data other than night time and high NO periods are due to instrument maintenance or malfunction.

Diurnal profiles of OH and $\text{HO}_2 + \text{RO}_2$ largely followed the patterns of $J(\text{O}^1\text{D})$ with a maximum at local noon, consistent with the behaviors of short-lived photochemically active species. Although 24 h of daylight are present in

summer time at Summit, $J(\text{O}^1\text{D})$ decreased by approximately a factor of 100 from noon to midnight. The maxima mid-day levels of OH and $\text{HO}_2 + \text{RO}_2$ increased as temperature, $J(\text{O}^1\text{D})$ and O_3 increased, which were consistent with the previous finding that O^1D reacting with H_2O and snow emissions of H_2O_2 were the dominant HO_x sources at Summit (Chen et al., 2007) (Mid-day is defined as 10:00–15:00 WGST). Overall, the maximum mid-day OH and $\text{HO}_2 + \text{RO}_2$ concentrations increased during the measurement period in spring 2007 as the summer solstice was approached. There was no significant trend in the maximum mid-day OH and $\text{HO}_2 + \text{RO}_2$ concentrations during summer 2008 (12 June 2008–8 July 2008) as the measurement period was centered about the solstice. The average mid-day OH and $\text{HO}_2 + \text{RO}_2$ concentrations were higher in summer 2008 than that in spring 2007, likely a result of the higher radiative fluxes ($J_{\text{O}_3-2007}/J_{\text{O}_3-2008} = 1:1.4$) and dew points in summer time. The midday median ratio of $\text{HO}_2 + \text{RO}_2$ to OH was 107:1 in spring 2007 and 102:1 in summer 2008 and the midday mean ratio of $\text{HO}_2 + \text{RO}_2$ to OH was 109:1 with a standard deviation of 23 in spring 2007 and 108:1 with a standard deviation of 37 in summer 2008. The $\text{HO}_2 + \text{RO}_2$ to OH ratios are comparable to other measurements performed in the lower troposphere in mid latitudes (Ren et al., 2008). The mid-day median and mean values of OH and $\text{HO}_2 + \text{RO}_2$ observations, as well as $J(\text{O}^1\text{D})$, $J(\text{NO}_2)$, NO, HNO_3 , HONO, O_3 , BrO, RGM and temperature in spring 2007 and summer 2008 are summarized in Table 3.

3.2 NO, HNO_3 and HONO observations

Diurnal profiles of NO and HONO were also observed at Summit. The average mid-day concentrations of NO and HONO were ~ 12 pptv and ~ 6 pptv, respectively. HONO levels were obtained from measurements of soluble nitrite (NO_2^-) from the mist chamber (Dibb et al., 2002). However, it should be noted that the derived HONO levels must be considered an upper limit to gas phase HONO as other species might also produce nitrite in solution. Following the simple NO_x and HONO lifetime arguments in Chen et al. (2004); NO levels of 12 ppt and HONO levels of 6 ppt would seem to indicate that the soluble nitrite measurement includes species other than HONO. Due to the increase of the boundary layer height through the day, the diurnal profiles of NO had a local minimum at noon (Thomas et al., 2011). Elevated HNO_3 was observed by mist chamber during the days when photochemically enhanced NO was observed. Higher NO, HNO_3 and HONO concentrations were observed in spring 2007 than in summer 2008.

3.3 RGM and GEM observations

Up to $\sim 250 \text{ pg m}^{-3}$ RGM were observed in the spring 2007 campaign. Clear diurnal profiles of RGM were observed when RGM was greater than 100 pg m^{-3} . Because bromine

atoms are one of the few established species that efficiently converts GEM into RGM (Ariya et al., 2002; Donohoue et al., 2006), elevated RGM peaks indicated that significant levels of BrO may be present. Higher RGM levels were observed in spring 2007 than in summer 2008, which suggests that the concentrations of BrO at Summit might be higher in spring 2007 than in summer 2008. High RGM appeared to coincide with photochemically enhanced NO and HNO_3 in most cases. This is consistent with snow photochemistry activating bromine chemistry as described in Thomas et al. (2011).

3.4 BrO observations

BrO mixing ratios detected by the LP DOAS ranged from below detection limit to 5.5 pptv with an average value of 1.6 pptv in 2007 at Summit. BrO was also measured by CIMS in the later period of the 2007 campaign with a mean value of 1.7 pptv, ranging from below detection limit to 6.4 pptv. Lower BrO mixing ratios were observed by both LP DOAS ($[\text{BrO}]_{\text{mean}} = 0.9$ pptv for all data available) and CIMS ($[\text{BrO}]_{\text{mean}} = 1.5$ pptv for all data available) in summer 2008. BrO mixing ratios in 2008 generally ranged from below detection limit to 4 pptv and 5 pptv detected by LP DOAS and CIMS respectively. To be noted, the BrO concentrations at Summit were often near detection limits of both instruments. Diurnal patterns of BrO were observed in spring 2007 and the early part (10 June to 13 June) of summer 2008 by the CIMS with maximum concentrations in the daytime, which is consistent with BrO as a photochemically active product. No significant diurnal patterns of BrO were observed by the CIMS in the later period of summer 2008 as the daytime BrO levels were near the detection limit.

4 Discussion

4.1 Model comparison

4.1.1 Base Model (BM)

The predicted OH and $\text{HO}_2 + \text{RO}_2$ from the BM are plotted against the observations in Fig. 4. Note that, the discrepancy between HO_x observations and predictions increased at high wind speeds ($\text{WS} > 8 \text{ m s}^{-1}$) and were excluded from the comparisons. On average 26 % of the HO_x data were excluded and the correlation coefficients were improved (R increase 0.03 on average for BM_model) when HO_x data were filtered at high wind speed conditions. Higher wind speed conditions did not clearly correspond to low photolysis rate or lower NO_x levels. The correlation coefficient (R) between photolysis rate and wind speeds were < 0.1 in 2007 and 2008. The correlation coefficient (R) between predicted NO_2 and wind speeds were -0.35 in 2007 and -0.29 in 2008. There is no clear systematic bias introduced when the HO_x data were filtered at high wind speeds but this filter excluded the

Table 2. Bromine reactions included in the HO_x model.

Reaction number	Reactions	Reaction rate coefficient k (cm ³ molec ⁻¹ s ⁻¹ or s ⁻¹)	$k(T = 250 \text{ K})$ (cm ³ molec ⁻¹ s ⁻¹ or s ⁻¹)
1	$\text{Br} + \text{O}_3 \rightarrow \text{BrO} + \text{O}_2$	$1.7 \times 10^{-11} \exp(-800/T)$	6.9×10^{-13}
2	$\text{BrO} + \text{HO}_2 \rightarrow \text{HOBr} + \text{O}_2$	$4.5 \times 10^{-12} \exp(460/T)$	2.8×10^{-11}
3a	$\text{BrO} + \text{BrO} \rightarrow 2\text{Br} + \text{O}_2$	$2.4 \times 10^{-12} \exp(40/T)$	2.8×10^{-12}
3b	$\rightarrow \text{Br}_2 + \text{O}_2$	$2.8 \times 10^{-14} \exp(860/T)$	8.7×10^{-13}
4	$\text{BrO} + \text{NO} \rightarrow \text{Br} + \text{NO}_2$	$8.8 \times 10^{-12} \exp(260/T)$	2.5×10^{-11}
5	$\text{BrO} + \text{NO}_2 + \text{M} \rightarrow \text{BrONO}_2 + \text{M}$	$k_0 = 5.2 \times 10^{-31} \exp(T/300)^{-3.2}$ $k_\infty = 6.9 \times 10^{-12} \exp(T/300)^{-2.9}$	5.3×10^{-12}
6	$\text{Br} + \text{CH}_2\text{O} \rightarrow \text{HBr} + \text{HCO}$	$1.7 \times 10^{-11} \exp(-800/T)$	6.9×10^{-13}
7	$\text{BrO} + h\nu \rightarrow \text{Br} + \text{O}$	0.06–0.08 (at noon)	
8	$\text{HOBr} + h\nu \rightarrow \text{Br} + \text{OH}$	$3 \times 10^{-3} - 4 \times 10^{-3}$ (at noon)	
9	Uptake of HOBr on heterogeneous surface	$\sim 1 \times 10^{-4}$	

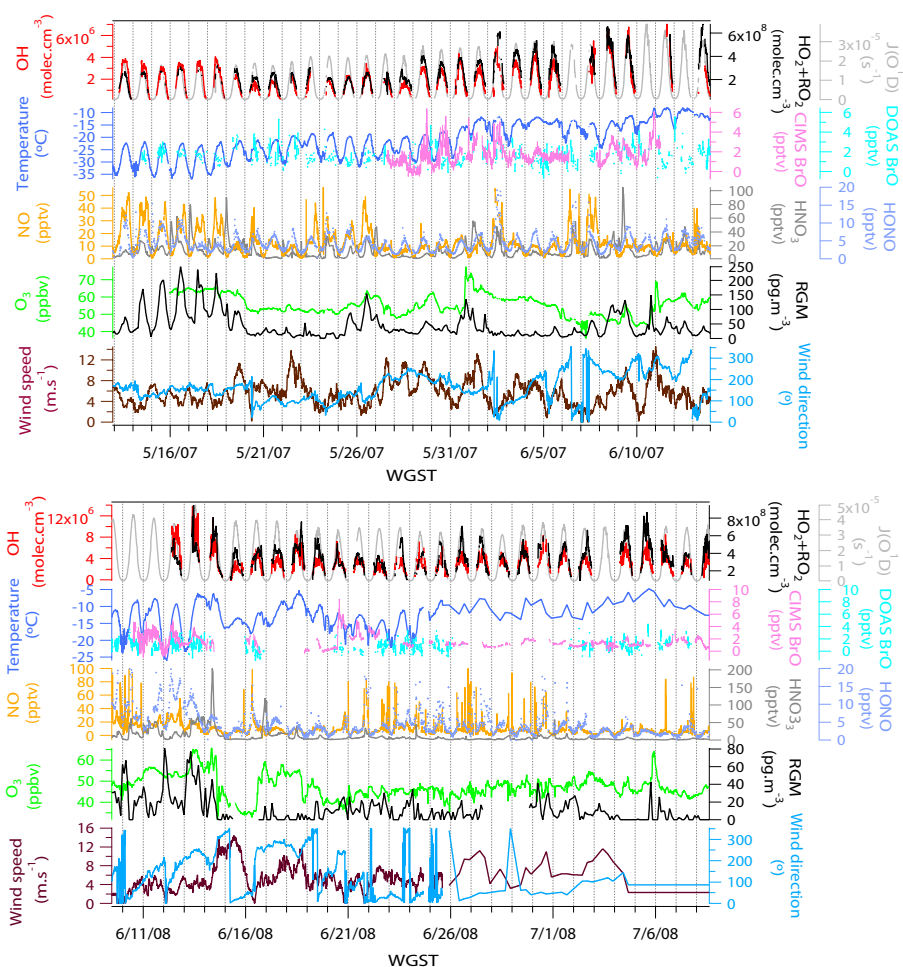
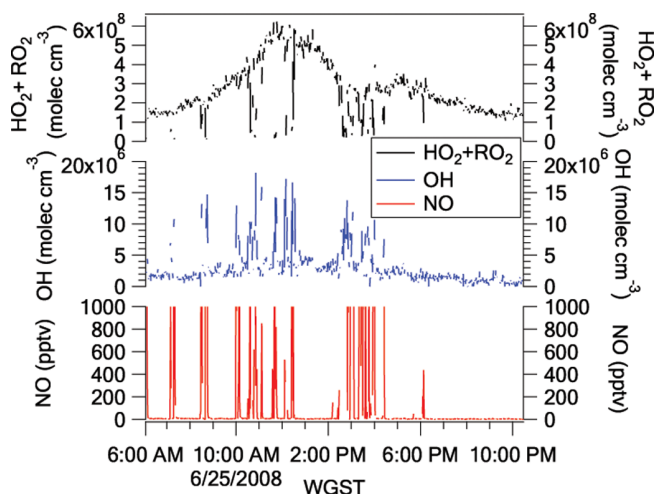
**Fig. 2.** Time series of measurements of HO₂ + RO₂, OH, $J(\text{O}^1\text{D})$, BrO, temperature, NO, HNO₃, HONO, O₃, RGM, wind speeds and directions on a 10 min time base in spring 2007 (top panel) and summer 2008 (bottom panel) Summit campaign.

Table 3. Photochemical species concentrations and parameters in the mid-day (10:00–15:00 WGST) at Summit, Greenland in 2007–2008. (Note: HO_x predictions are from the base model.)

Species	Year 2007 (13 May–13 June)		Year 2008 (10 June–8 July)	
	Median	Average	Median	Average
OH (10^6 molec cm ⁻³)	3.0	3.1	4.1	4.6
HO ₂ + RO ₂ (10^8 molec cm ⁻³)	2.7	3.3	4.2	4.4
OH pred (10^6 molec cm ⁻³)	2.4	2.6	3.7	3.8
HO ₂ + RO ₂ pred (10^8 molec cm ⁻³)	3.0	3.2	4.6	4.6
NO (pptv)	12.8	17.2	8.6	11.4
O ₃ (ppbv)	54.6	55.3	47.3	47.9
BrO _L PDOAS (pptv)	1.5	1.6	1.0	0.9
BrO _{CIMS} (pptv)	1.8	2.0	1.5	2.0
RGM (pg m ⁻³)	41.8	64.8	7.2	9.6
HNO ₃ (pptv)	12.9	15.9	5.5	11.5
HONO (pptv)	6.5	7.3	4.7	5.8
<i>J</i> (O ¹ D) (10^{-5} s ⁻¹)	2.2	2.3	3.3	3.3
<i>J</i> NO ₂ (s ⁻¹)	0.014	0.014	0.016	0.016
Temperature (°C)	−19.5	−18.2	−10.7	−10.6

**Fig. 3.** An example of elevated OH and depleted HO₂ + RO₂ at high NO conditions. The spikes in NO and the responses in OH and HO₂ + RO₂ are due to the measurement site being impacted by the plume of the generator.

most scattered points. It is possible that the uncertainty in the CIMS calibration increases at high wind speeds (>8 m s⁻¹) due to turbulent flow in the inlet as suggested in Sjøstedt et al. (2007). Overall, the observed and predicted OH and HO₂ + RO₂ from the BM were well correlated (HO₂ + RO₂: $R = 0.90$, OH: $R = 0.83$ in 2007; HO₂ + RO₂: $R = 0.79$, OH: $R = 0.76$ in 2008). The BM well predicted the magnitude of HO₂ + RO₂ and under predicted OH, especially in summer 2008 (HO₂ + RO₂: slope = 0.87, OH: slope = 0.72 in

2007; HO₂ + RO₂: slope = 0.96, OH: slope = 0.54 in 2008). The slopes were given by equally weighted bivariate regressions. The agreement between the predicted and observed HO₂ + RO₂ (which is dominated by HO₂) indicates that we have a good understanding of the major sources and sinks of HO₂ which dominates the HO_x family. However, our understanding of the OH sources and sinks is clearly lacking especially during periods of elevated RGM (see Sect. 4.4). The model predicted an average midday HO₂ + RO₂ to OH ratio of 121:1 in 2007 and 125:1 in 2008, consistent with the values predicted by Chen et al. (2007) using input data from the summit 2003 campaign. The observed average midday HO₂ + RO₂ to OH ratios were 109:1 in 2007 and 108:1 in 2008. The predicted and observed HO₂ + RO₂ to OH ratios indicate that a mechanism rolling HO₂ back to OH may be missing, with halogen chemistry a likely prospect.

4.1.2 Base Model constrained to HONO measurements (BM.HONO)

The correlation coefficients and slopes between predictions from the BM.HONO and observations are shown in Fig. 5 (HO₂ + RO₂: $R = 0.84$, slope = 0.90 in 2007 and $R = 0.79$, slope = 1.09 in 2008; OH: $R = 0.78$, slope = 0.92 in 2007 and $R = 0.78$, slope = 0.72 in 2008). The slopes were given by equally weighted bivariate regressions. The correlation coefficient (R) between predicted and observed HO_x did not improve when the model included HONO source. In 2007, the average modeled to observed (M/O) ratios of HO₂ + RO₂ and OH were 0.87 and 0.84 from the BM, and were 1.18 and 1.25 from the BM.HONO. In 2008, the average M/O ratios

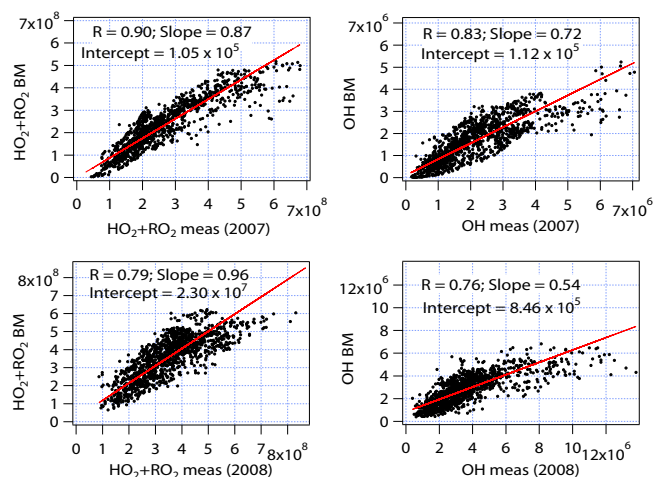


Fig. 4. HO₂ + RO₂ and OH predictions from the base model (BM) plotted versus the observations in 2007 and 2008. The data are average on a 10 min time base. The correlation coefficient (*R*) and the slope and intercept from an equally weighted bivariate regression (red line) for each panel are also denoted in the figure. The units of OH and HO₂ + RO₂ concentrations are molec cm⁻³.

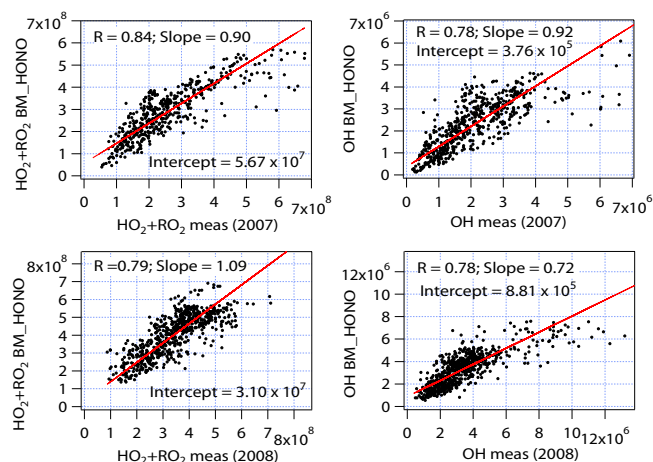


Fig. 5. HO₂ + RO₂ and OH predictions from the base model constrained to HONO measurements (BM_HONO) plotted versus the observations in 2007 and 2008. The data are average on a 10 min time base. The correlation coefficient (*R*) and the slope and intercept from an equally weighted bivariate regression (red line) for each panel are also denoted in the figure. The units of OH and HO₂ + RO₂ concentrations are molec cm⁻³.

of HO₂ + RO₂ and OH were 1.06 and 0.87 from the BM, and were 1.22 and 1.05 from the BM_HONO. The predictions of both OH and HO₂ + RO₂ from the BM_HONO were higher than that from the BM as this adds in a HO_x source. However, the ratio of HO₂ + RO₂ to OH changed by less than 10 % on average. As the HO_x predictions from the BM had more data points, the correlation between predicted and observed HO_x did not improve when HONO was included in

the model, and the observed HONO is likely to have interferences (Stutz et al., 2010; Sjostedt et al., 2007), the BM is preferred for comparison to HO_x observations in this work.

4.1.3 Model incorporating halogen chemistry (BM_BrO)

To investigate the impact of BrO on HO_x, predicted OH and HO₂ + RO₂ from the BM_BrO unconstrained by HONO measurements and constrained by BrO measurements from the CIMS (BM_BrO_{CIMS}) and LP DOAS (BM_BrO_{LPDOAS}) in 2007 and 2008 are also plotted against the observations (Fig. 6). Overall, the correlation coefficients between the observed and predicted OH and HO₂ + RO₂ were slightly improved (increased 0.03 except HO₂ + RO₂ in 2007) by incorporation of bromine chemistry with the BrO constrained to the CIMS observations. When the model included bromine chemistry and was constrained to CIMS BrO, the intercept increased from 1.12×10^5 molec cm⁻³ to 1.65×10^5 molec cm⁻³ and the slope increased from 0.72 to 0.78 in 2007 and the intercept increased from 8.46×10^5 molec cm⁻³ to 9.23×10^5 molec cm⁻³ and the slope increased from 0.54 to 0.56 in 2008 for OH. When the model included bromine chemistry and was constrained to LPDOAS BrO, the intercepts increased from 1.12×10^5 molec cm⁻³ to 3.20×10^5 molec cm⁻³ and the slope remained the same in 2007 and the intercept increased from 8.46×10^5 molec cm⁻³ to 1.15×10^6 molec cm⁻³ and the slope slightly decreased from 0.54 to 0.50 in 2008 for OH. To give a general idea of the difference between predicted OH and HO₂ + RO₂ from the BM and BM_BrO, the average ratios of OH and HO₂ + RO₂ from both models as well as the slopes and intercepts from linear equally weighted bivariate regression are also provided. Predicted OH increased 12 % ($[\text{OH}]_{\text{pred_BrO_CIMS}}/[\text{OH}]_{\text{pred_avg}}$) in 2007 and 10 % in 2008, and predicted HO₂ + RO₂ decreased 10 % in 2007 and 8 % in 2008 on average when the BM_BrO was constrained to CIMS BrO. Predicted OH increased 10 % in 2007 and 4 % in 2008, and predicted HO₂ + RO₂ decreased 8 % in 2007 and 3 % in 2008 on average when the BM_BrO was constrained to LP DOAS BrO. These results indicate that BrO impacted the concentrations of OH and HO₂ + RO₂ at Summit, although all of the enhancement in observed OH relative to model predictions cannot be explained by the influence of BrO.

4.1.4 Impact of H₂O₂ and CH₂O

Because CH₂O and H₂O₂ were not observed, they had to be predicted with the photochemical model which may lead to under estimation of them as they are emitted to the atmosphere from the snowpack (Hutterli et al., 1999, 2001). Under estimation of CH₂O and H₂O₂ results in under prediction of OH and HO₂ + RO₂, but does not significantly impact the ratios of OH/ HO₂ + RO₂. For example, a 30 % increase in

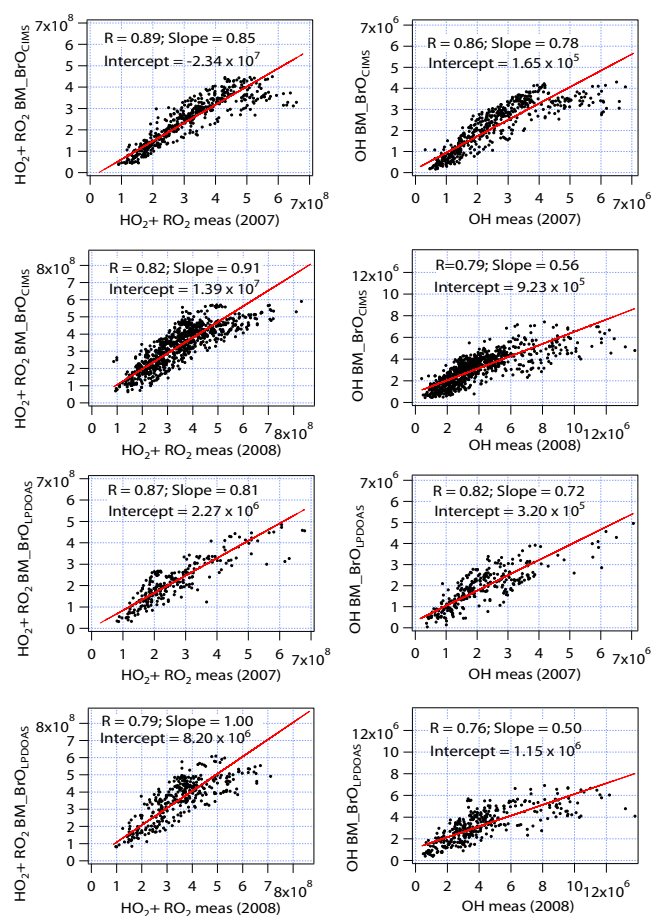


Fig. 6. HO₂ + RO₂ and OH predictions from the base model incorporating bromine chemistry constrained by BrO measurements by CIMS (BM.BrO_{CIMS}) and LPDOAS (BM.BrO_{LPDOAS}) plotted versus the observations in 2007 and 2008. The data are averaged on a 10 min time base. The correlation coefficient (*R*) and the slope and intercept from an equally weighted bivariate regression (red line) for each panel are also denoted in the figure. The units of OH and HO₂ + RO₂ concentrations are molec cm⁻³.

the model production rate of H₂O₂ or CH₂O would increase HO_x levels by ~5 % and ~10 % but would impact the ratio of OH to RO₂ by less than 2 %. According to the study of HO_x at Summit in 2003 by Chen et al. (2007), H₂O₂ is the largest snow emitted HO_x sources at Summit, contributing to 37 % of the net HO_x sources compared to only 3 % from CH₂O. As snow emissions of H₂O₂ increase with temperature (Chen et al., 2007), the warmer temperature in summer 2008 may have contributed to the lower correlation between predicted and observed HO_x in that year. For this reason, temperature dependent snow emissions of H₂O₂, based on net snow-air exchange rate shown as the following equation, were added to the BM.

$$d[\text{H}_2\text{O}_2]/dt = A \times \exp(B/\text{Temperature}_{\text{snow}}) - C \times [\text{H}_2\text{O}_2](\text{molec cm}^{-3} \text{ s}^{-1} \text{ or ppbv hr}^{-1})$$

A, *B* and *C* are adjustable constants. Temperature is assumed to be ambient temperature instead of snow temperature. [H₂O₂] represents ambient H₂O₂ concentration (Chen et al., 2007). No significant improvement of the correlation was found between predicted and observed HO_x. However, as observations of H₂O₂ and CH₂O were not carried out in 2007 or 2008, enhanced snow photochemistry producing these and potentially other radical precursors in 2008 cannot be ruled out.

4.2 Average comparison

Figure 7 shows the average diurnal profiles of hourly OH and HO₂ + RO₂ concentrations from observations and predictions from the BM and the BM.BrO constrained to CIMS measurements in 2007 and 2008. The error bars of the observations are the overall uncertainties including the measurement uncertainties and ambient fluctuations. The error bars of the predictions are the propagated uncertainties from the model inputs uncertainties and variations. The BM simulated the concentrations of OH and HO₂ + RO₂ within the combined uncertainties, except for the OH concentrations in the late afternoons in summer 2008. This confirms that the BM captures the dominant HO_x sources and sinks. The BM also under predicts the OH concentrations in both 2007 and 2008. The midday median modeled to observed (M/O) ratio of OH was 0.88 and 0.87 in 2007 and 2008, and the mid-day median M/O ratio of HO₂ + RO₂ was 0.97 and 1.08 in 2007 and 2008. A low M/O ratio of OH was also reported in Sjostedt et al. (2007). The average hourly HO₂ + RO₂ and OH predictions from the BM.BrO constrained to CIMS BrO measurements in 2007 slightly over estimated their concentrations due to the absence of CIMS BrO measurements in the early period of the 2007 campaign and the increase in HO_x levels in the late period of the 2007 campaign relative to the early period. The OH concentrations predicted from BM.BrO were higher compared to the results from the BM, and the average hourly predicted HO₂ + RO₂ concentrations slightly decreased when BM incorporated bromine chemistry in 2008. The model including bromine chemistry brought the predictions both of OH and HO₂ + RO₂ closer to the observations in 2008. The impact of bromine chemistry on HO₂ + RO₂ concentrations was smaller than on OH concentrations. The box model consistently under predicts the OH concentrations in the later afternoons, which indicates that box model underestimates the sources of OH as the radiation flux and boundary layer height decrease or there may be a change in the sinks or cycling. A similar behavior was observed by Sjostedt et al. (2007). Snow emitted compounds with higher concentrations or steeper vertical gradients in the later afternoon not included in the photochemical box model may contribute to the under predictions of OH and impact the photochemistry at Summit in the later afternoon.

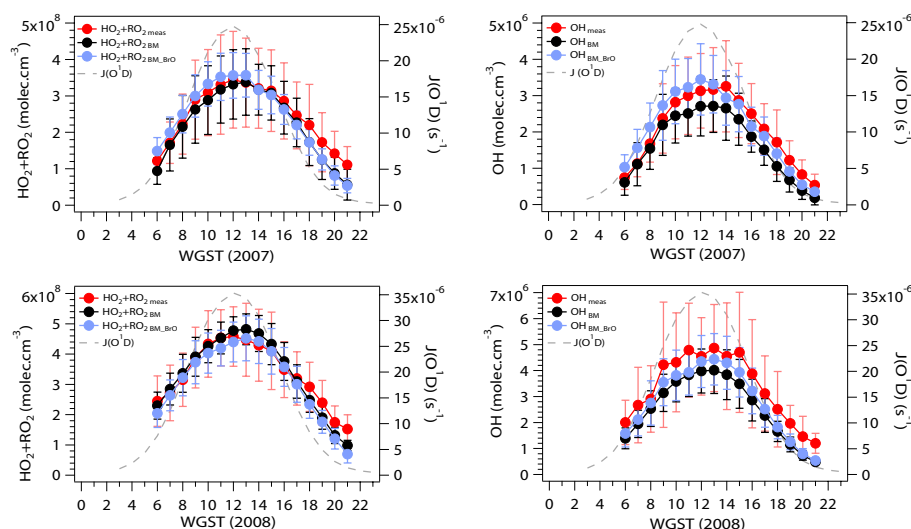


Fig. 7. The average diurnal profiles of hourly OH and $\text{HO}_2 + \text{RO}_2$ observations (red dots and line) and predictions from the BM (black dots and line) and BM.BrOCIMS (blue dots and line), and diurnal profile of $J(\text{O}^1\text{D})$ (gray dash line) in spring 2007 and summer 2008. The error bars (red) of the observations are the overall uncertainties including the measurement uncertainties and ambient fluctuations. The error bars (gray and blue) of the predictions are the propagated uncertainties from the model input uncertainties and variations.

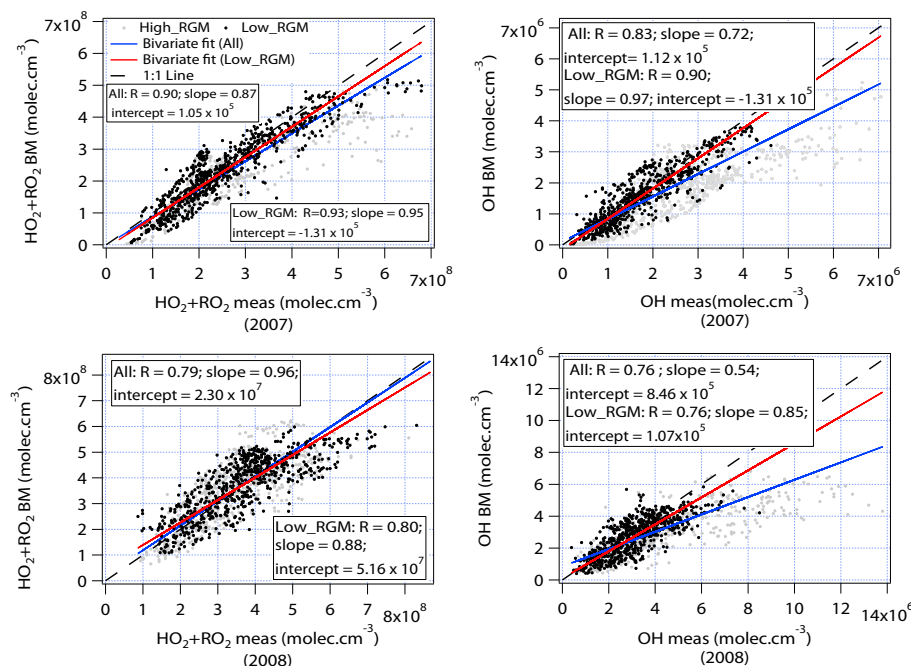


Fig. 8. The correlation plots of observed and predicted OH and $\text{HO}_2 + \text{RO}_2$ from the BM at low RGM conditions (black dots) and at high RGM conditions (gray dots) in 2007 and 2008. “All” represents the total data including low RGM and high RGM conditions. Equally weighted bivariate regressions are applied to all the data (blue line) and the data at low RGM conditions (red line), respectively. The relevant correlation coefficients, slopes, and intercepts are provided in the figure.

4.3 Enhanced OH and RGM

Due to the limitations of BrO measurements discussed earlier, observations of RGM were also investigated as a proxy for bromine and potentially other chemistry. The correlations

between the BM predictions and observations of HO_x were examined for enhanced RGM levels (gray dots in Fig. 8) and low RGM levels (black dots in Fig. 8). RGM levels were considered to be enhanced when they were above average levels

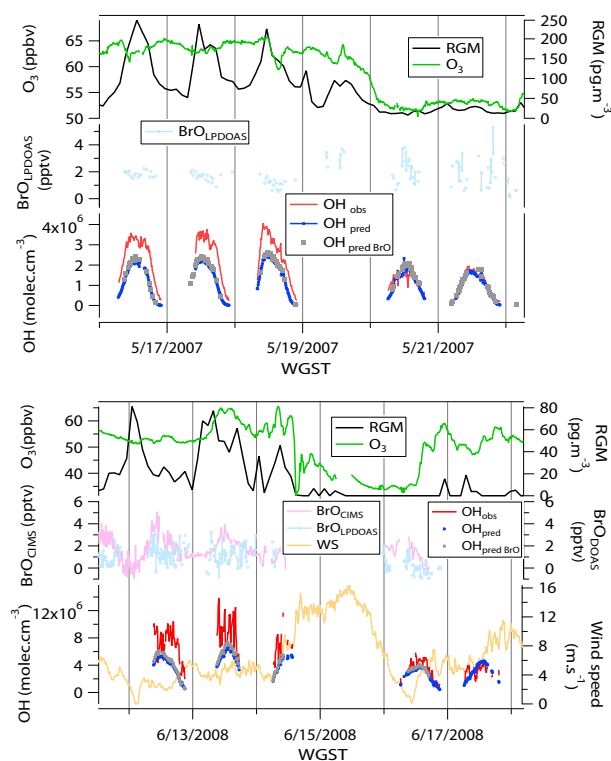


Fig. 9. (a): Observations of RGM, O_3 , BrO by DOAS and OH, and predictions of OH from the BM and BM.BrO when enhanced RGM were observed in 2007 (16 May–21 May 2007); (b): The observations of RGM, O_3 , OH, wind speeds, BrO by CIMS and DOAS, and the predictions of OH from the BM and BM.BrO when enhanced RGM were observed in 2008 (11 June–17 June 2008).

for each of the field seasons and season means were 45 and 11 pg m^{-3} in 2007 and 2008, respectively.

When high RGM periods were excluded, the slope between the predicted and observed OH significantly increased: the slope of OH increased from 0.72 to 0.97 in 2007 and increased from 0.54 to 0.85 in 2008. The correlation between the predicted and observed OH and $\text{HO}_2 + \text{RO}_2$ in 2007 also slightly improved: the correlation coefficient increased from 0.83 to 0.90 for OH and increased from 0.90 to 0.93 for $\text{HO}_2 + \text{RO}_2$. For the 2008 data the correlation was essentially unchanged when high RGM periods were excluded. These results indicate that OH levels are enhanced above predictions when RGM is enhanced. This is consistent with other chemistry (e.g. other halogens) coincident with the Br chemistry that leads to elevated RGM impacting the production of OH from HO_2 and RO_2 .

4.4 Case study with high RGM

The concentrations of OH, O_3 , RGM, and BrO during two periods (16 May–21 May 2007; 12 June–17 June 2008) are shown in Fig. 9. The BM clearly under predicted OH during 16 May–18 May 2007 (Fig. 9a). Clear diurnal profiles

of RGM were present during the same period, with a maximum concentration of near 250 pg m^{-3} . The RGM peaks indicate that certain levels of Br and BrO may be present during these periods. Small O_3 concentration drops also occurred with the RGM peaks, possibly a result of bromine catalyzed O_3 depletion. Up to 5 pptv of BrO were observed by LP DOAS and no CIMS BrO measurements were available during this time. OH predictions from BM.BrO constrained by LP DOAS BrO measurements cannot account for the enhanced OH observed.

Figure 9b shows the early period of 2008 campaign including three days (12 June–14 June 2008) with obvious under prediction of OH. The RGM peaks during this period were the highest values in 2008 campaign with a maximum of $\sim 80 \text{ pg m}^{-3}$. During this period, up to $4\text{--}5 \text{ pptv}$ of BrO were observed by CIMS, and up to $\sim 3 \text{ pptv}$ of BrO were observed by LP DOAS. The BrO levels were near the detection limits of the LP DOAS and CIMS instruments. The gaps of BrO and HO_x measurements during 12 June–14 June 2008 were due to the extremely high wind speeds ($> 12 \text{ m s}^{-1}$). The OH predictions from BM.BrO constrained by CIMS BrO measurements are also shown in Fig. 9b. These levels of BrO were not large enough to explain the under prediction of OH. The BrO concentrations during 12 June–14 June 2008 only contribute $\sim 10\%$ to the OH production rate.

5 Conclusions

The median midday values of $\text{HO}_2 + \text{RO}_2$ and OH concentrations observed by CIMS were $2.7 \times 10^8 \text{ molec cm}^{-3}$ and $3.0 \times 10^6 \text{ molec cm}^{-3}$ in spring 2007, and $4.2 \times 10^8 \text{ molec cm}^{-3}$ and $4.1 \times 10^6 \text{ molec cm}^{-3}$ in summer 2008 at Summit. The BM was reasonably accurate for $\text{HO}_2 + \text{RO}_2$ ($R = 0.90$, slope = 0.87 in 2007; $R = 0.79$, slope = 0.96 in 2008) but under predicted OH ($R = 0.83$, slope = 0.72 in 2007; $R = 0.76$, slope = 0.54 in 2008). This confirmed our understanding of the dominant HO_x sources and sinks in this environment and that there may be mechanisms perturbing HO_x cycling and enhancing OH above the snow pack. Inclusion of HONO source in the model did not impact the correlation between predictions and observations of HO_x significantly and did not improve the ratio of OH to $\text{HO}_2 + \text{RO}_2$. BrO levels detected by CIMS and LP DOAS generally ranged from below detection limits to $\sim 6 \text{ pptv}$ and $\sim 5 \text{ pptv}$, respectively. The correlation between observed and predicted $\text{HO}_2 + \text{RO}_2$ and OH from the BM.BrO_{CIMS} slightly improved relative to the BM. The model incorporating bromine chemistry brought the average hourly OH and $\text{HO}_2 + \text{RO}_2$ predictions closer to the observations in 2008. This indicates that BrO at Summit impacted the HO_x levels, although most of the discrepancies between observations and models cannot be explained by the influence of detected BrO. High levels of RGM were found to be coincident with the significant under predictions of OH, and exclusion of high RGM periods significantly increased the agreement

between predicted and observed OH. This is consistent with bromine chemistry and potentially other chemistry leading to elevated RGM and impacting the production OH from HO₂ and RO₂. Enhanced snow photochemistry producing H₂O₂, CH₂O and potentially other radical precursors at higher temperature may have contributed to the larger discrepancy between predicted and observed HO_x in summer 2008.

Acknowledgements. This work is financially supported by NSF GEO ATM Tropospheric Chemistry program (Grant ATM-0612279:002). We thank NSF OPP, CH2MHill Polar Services, and the 109th Air National Guard for logistical support. We also thank Greenland Home rule for permission to work at Summit.

Edited by: J. Abbatt

References

- Ariya, P. A., Khalizov, A., and Gidas, A.: Reactions of gaseous mercury with atomic and molecular halogens: Kinetics, product studies, and atmospheric implications, *J. Phys. Chem. A*, 106, 7310–7320, doi:10.1021/jp020719o, 2002.
- Bloss, W. J., Lee, J. D., Heard, D. E., Salmon, R. A., Bauguutte, S. J.-B., Roscoe, H. K., and Jones, A. E.: Observations of OH and HO₂ radicals in coastal Antarctica, *Atmos. Chem. Phys.*, 7, 4171–4185, doi:10.5194/acp-7-4171-2007, 2007.
- Bloss, W. J., Camredon, M., Lee, J. D., Heard, D. E., Plane, J. M. C., Saiz-Lopez, A., Bauguutte, S. J.-B., Salmon, R. A., and Jones, A. E.: Coupling of HO_x, NO_x and halogen chemistry in the antarctic boundary layer, *Atmos. Chem. Phys.*, 10, 10187–10209, doi:10.5194/acp-10-10187-2010, 2010.
- Brooks, S., Arimoto, R., Lindberg, S., and Southworth, G.: Antarctic polar plateau snow surface conversion of deposited oxidized mercury to gaseous elemental mercury with fractional long-term burial, *Atmos. Environ.*, 42, 2877–2884, doi:10.1016/j.atmosenv.2007.05.029, 2008.
- Brooks, S., Moore, C., Lew, D., Lefer, B., Huey, G., and Tanner, D.: Temperature and sunlight controls of mercury oxidation and deposition atop the Greenland ice sheet, *Atmos. Chem. Phys. Discuss.*, 11, 3663–3691, doi:10.5194/acpd-11-3663-2011, 2011.
- Chen, G., Davis, D., Crawford, J., Nowak, J. B., Eisele, F., Mauldin, R. L., Tanner, D., Buhr, M., Shetter, R., Lefer, B., Arimoto, R., Hogan, A., and Blake, D.: An investigation of South Pole HO_x chemistry: Comparison of model results with ISCAT observations, *Geophys. Res. Lett.*, 28, 3633–3636, 2001.
- Chen, G., Davis, D., Crawford, J., Hutterli, L. M., Huey, L. G., Slusher, D., Mauldin, L., Eisele, F., Tanner, D., Dibb, J., Buhr, M., McConnell, J., Lefer, B., Shetter, R., Blake, D., Song, C. H., Lombardi, K., and Arnoldy, J.: A reassessment of HO_x South Pole chemistry based on observations recorded during ISCAT 2000, *Atmos. Environ.*, 38, 5451–5461, doi:10.1016/j.atmosenv.2003.07.018, 2004.
- Chen, G., Huey, L. G., Crawford, J. H., Olson, J. R., Hutterli, M. A., Sjostedt, S., Tanner, D., Dibb, J., Lefer, B., Blake, N., Davis, D., and Stohl, A.: An assessment of the polar HO_x photochemical budget based on 2003 Summit Greenland field observations, *Atmos. Environ.*, 41, 7806–7820, doi:10.1016/j.atmosenv.2007.06.014, 2007.
- Crawford, J. H., Davis, D. D., Chen, G., Buhr, M., Oltmans, S., Weller, R., Mauldin, L., Eisele, F., Shetter, R., Lefer, B., Arimoto, R., and Hogan, A.: Evidence for photochemical production of ozone at the South Pole surface, *Geophys. Res. Lett.*, 28, 3641–3644, 2001.
- Davis, D., Nowak, J. B., Chen, G., Buhr, M., Arimoto, R., Hogan, A., Eisele, F., Mauldin, L., Tanner, D., Shetter, R., Lefer, B., and McMurtry, P.: Unexpected high levels of NO observed at South Pole, *Geophys. Res. Lett.*, 28, 3625–3628, 2001.
- Dibb, J. E. and Jaffrezo, J. L.: Air-snow exchange investigations at Summit, Greenland: An overview, *J. Geophys. Res.-Ocean.*, 102, 26795–26807, 1997.
- Dibb, J. E., Arsenault, M., Peterson, M. C., and Honrath, R. E.: Fast nitrogen oxide photochemistry in Summit, Greenland snow, *Atmos. Environ.*, 36, 2501–2511, 2002.
- Dibb, J. E., Huey, L. G., Slusher, D. L., and Tanner, D. J.: Soluble reactive nitrogen oxides at South Pole during ISCAT 2000, *Atmos. Environ.*, 38, 5399–5409, doi:10.1016/j.atmosenv.2003.01.001, 2004.
- Donohoue, D. L., Bauer, D., Cossairt, B., and Hynes, A. J.: Temperature and pressure dependent rate coefficients for the reaction of Hg with Br and the reaction of Br with Br: A pulsed laser photolysis-pulsed laser induced fluorescence study, *J. Phys. Chem. A*, 110, 6623–6632, doi:10.1021/jp054688j, 2006.
- Edwards, G. D., Cantrell, C. A., Stephens, S., Hill, B., Goyea, O., Shetter, R. E., Mauldin, R. L., Kosciuch, E., Tanner, D. J., and Eisele, F. L.: Chemical ionization mass spectrometer instrument for the measurement of tropospheric HO₂ and RO₂, *Anal. Chem.*, 75, 5317–5327, doi:10.1021/ac034402b, 2003.
- Faïn, X., Ferrari, C. P., Dommergue, A., Albert, M., Battle, M., Arnaud, L., Barnola, J.-M., Cairns, W., Barbante, C., and Boutron, C.: Mercury in the snow and firn at Summit Station, Central Greenland, and implications for the study of past atmospheric mercury levels, *Atmos. Chem. Phys.*, 8, 3441–3457, doi:10.5194/acp-8-3441-2008, 2008.
- Grannas, A. M., Jones, A. E., Dibb, J., Ammann, M., Anastasio, C., Beine, H. J., Bergin, M., Bottenheim, J., Boxe, C. S., Carver, G., Chen, G., Crawford, J. H., Dominé, F., Frey, M. M., Guzmán, M. I., Heard, D. E., Helmig, D., Hoffmann, M. R., Honrath, R. E., Huey, L. G., Hutterli, M., Jacobi, H. W., Klán, P., Lefer, B., McConnell, J., Plane, J., Sander, R., Savarino, J., Shepson, P. B., Simpson, W. R., Sodeau, J. R., von Glasow, R., Weller, R., Wolff, E. W., and Zhu, T.: An overview of snow photochemistry: evidence, mechanisms and impacts, *Atmos. Chem. Phys.*, 7, 4329–4373, doi:10.5194/acp-7-4329-2007, 2007.
- Haman, C., Lefer, B., Dibb, J. E., and Clements, C.: Evidence for a mid- to upper-tropospheric source of bromide reaching Summit, *Atmos. Chem. Phys. Discuss.*, in preparation, 2011.
- Hammer, C. U., Clausen, H. B., and Dansgaard, W.: Greenland ice-sheet evidence of post-glacial volcanism and its climatic impact, *Nature*, 288, 230–235, 1980.
- Hausmann, M. and Platt, U.: Spectroscopic measurement of bromine oxide and ozone in the high Arctic during polar sunrise experiment 1992, *J. Geophys. Res.-Atmos.*, 99, 25399–25413, 1994.
- Helmig, D., Boulter, J., David, D., Birks, J. W., Cullen, N. J., Steffen, K., Johnson, B. J., and Oltmans, S. J.: Ozone and meteorological Summit, Greenland, boundary-layer conditions at during 3–21 June 2000, *Atmos. Environ.*, 36, 2595–2608, 2002.

- Helmig, D., Johnson, B. J., Warshawsky, M., Morse, T., Neff, W. D., Eisele, F., and Davis, D. D.: Nitric oxide in the boundary-layer at South Pole during the Antarctic Tropospheric Chemistry Investigation (ANTCI), *Atmos. Environ.*, 42, 2817–2830, doi:10.1016/j.atmosenv.2007.03.061, 2008.
- Honrath, R. E., Peterson, M. C., Guo, S., Dibb, J. E., Shepson, P. B., and Campbell, B.: Evidence of NO_x production within or upon ice particles in the Greenland snowpack, *Geophys. Res. Lett.*, 26, 695–698, 1999.
- Honrath, R. E., Lu, Y., Peterson, M. C., Dibb, J. E., Arsenault, M. A., Cullen, N. J., and Steffen, K.: Vertical fluxes of NO_x, HONO, and HNO₃ above the snowpack at Summit, Greenland, *Atmos. Environ.*, 36, 2629–2640, 2002.
- Huey, L. G., Hanson, D. R., and Howard, C. J.: Reactions of SF₆[−] and I[−] with atmospheric trace gases, *J. Phys. Chem.*, 99, 5001–5008, 1995.
- Huey, L. G., Tanner, D. J., Slusher, D. L., Dibb, J. E., Arimoto, R., Chen, G., Davis, D., Buhr, M. P., Nowak, J. B., Mauldin, R. L., Eisele, F. L., and Kosciuch, E.: CIMS measurements of HNO₃ and SO₂ at the South Pole during ISCAT 2000, *Atmos. Environ.*, 38, 5411–5421, doi:10.1016/j.atmosenv.2004.04.037, 2004.
- Hutterli, M. A., Rothlisberger, R., and Bales, R. C.: Atmosphere-to-snow-to-firn transfer studies of HCHO at Summit, Greenland, *Geophys. Res. Lett.*, 26, 1691–1694, 1999.
- Hutterli, M. A., McConnell, J. R., Stewart, R. W., Jacobi, H. W., and Bales, R. C.: Impact of temperature-driven cycling of hydrogen peroxide (H₂O₂) between air and snow on the planetary boundary layer, *J. Geophys. Res.-Atmos.*, 106, 15395–15404, 2001.
- Hutterli, M. A., McConnell, J. R., Chen, G., Bales, R. C., Davis, D. D., and Lenschow, D. H.: Formaldehyde and hydrogen peroxide in air, snow and interstitial air at South Pole, *Atmos. Environ.*, 38, 5439–5450, doi:10.1016/j.atmosenv.2004.06.003, 2004.
- Jefferson, A., Tanner, D. J., Eisele, F. L., Davis, D. D., Chen, G., Crawford, J., Huey, J. W., Torres, A. L., and Berresheim, H.: OH photochemistry and methane sulfonic acid formation in the coastal Antarctic boundary layer, *J. Geophys. Res.-Atmos.*, 103, 1647–1656, 1998.
- Jones, A. E., Wolff, E. W., Salmon, R. A., Bauguutte, S. J.-B., Roscoe, H. K., Anderson, P. S., Ames, D., Clemittshaw, K. C., Fleming, Z. L., Bloss, W. J., Heard, D. E., Lee, J. D., Read, K. A., Hamer, P., Shallcross, D. E., Jackson, A. V., Walker, S. L., Lewis, A. C., Mills, G. P., Plane, J. M. C., Saiz-Lopez, A., Sturges, W. T., and Worton, D. R.: Chemistry of the Antarctic Boundary Layer and the Interface with Snow: an overview of the CHABLIS campaign, *Atmos. Chem. Phys.*, 8, 3789–3803, doi:10.5194/acp-8-3789-2008, 2008.
- Kim, S., Huey, L. G., Stickel, R. E., Tanner, D. J., Crawford, J. H., Olson, J. R., Chen, G., Brune, W. H., Ren, X., Leshner, R., Wooldridge, P. J., Bertram, T. H., Perring, A., Cohen, R. C., Lefer, B. L., Shetter, R. E., Avery, M., Diskin, G., and Sokolik, I.: Measurement of HO₂NO₂ in the free troposphere during the intercontinental chemical transport experiment – North America 2004, *J. Geophys. Res.-Atmos.*, 112, D12s01, doi:10.1029/2006jd007676, 2007.
- Liao, J., Sihler, H., Huey, L. G., Neuman, J. A., Tanner, D. J., Friess, U., Platt, U., Flocke, F. M., Orlando, P. B., Shepson, J. J., Beine, H. J., Weinheimer, A. J., Sjostedt, S. J., Nowak, J. B., Knapp, D. J., Staebler, R. M., Zheng, W., Sander, R., Hall, S. R., and Ullman, K.: A comparison of Arctic BrO measurements by chemical ionization mass spectrometry (CIMS) and long path-differential optical absorption spectroscopy (LP-DOAS), *J. Geophys. Res.*, 116, D00R02, doi:10.1029/2010JD014788, 2011a.
- Liao, J., Huey, L. G., Tanner, D. J., Flocke, F. M., Orlando, J. J., Neuman, J. A., Nowak, J. B., Weinheimer, A. J., Hall, S. R., Smith, J. N., Fried, A., Staebler, R. M., Wang, Y., Koo, J.-H., Cantrell, C. A., Weibring, P., Walega, J., Knapp, D. J., Shepson, P. B., and Stephens, C. R.: Observed and modeled inorganic bromine (HOBr, BrO, and Br₂) speciation at Barrow, AK in spring 2009, *J. Geophys. Res.*, in review, 2011b.
- Mahajan, A. S., Oetjen, H., Lee, J. D., Saiz-Lopez, A., McFiggans, G. B., and Plane, J. M. C.: High bromine oxide concentrations in the semi-polluted boundary layer, *Atmos. Environ.*, 43, 3811–3818, doi:10.1016/j.atmosenv.2009.05.033, 2009.
- Mao, J., Jacob, D. J., Evans, M. J., Olson, J. R., Ren, X., Brune, W. H., St. Clair, J. M., Crounse, J. D., Spencer, K. M., Beaver, M. R., Wennberg, P. O., Cubison, M. J., Jimenez, J. L., Fried, A., Weibring, P., Walega, J. G., Hall, S. R., Weinheimer, A. J., Cohen, R. C., Chen, G., Crawford, J. H., McNaughton, C., Clarke, A. D., Jaegle, L., Fisher, J. A., Yantosca, R. M., Le Sager, P., and Carouge, C.: Chemistry of hydrogen oxide radicals (HO_x) in the Arctic troposphere in spring, *Atmos. Chem. Phys.*, 10, 5823–5838, doi:10.5194/acp-10-5823-2010, 2010.
- Mauldin, R. L., Eisele, F. L., Tanner, D. J., Kosciuch, E., Shetter, R., Lefer, B., Hall, S. R., Nowak, J. B., Buhr, M., Chen, G., Wang, P., and Davis, D.: Measurements of OH, H₂SO₄, and MSA at the South Pole during ISCAT, *Geophys. Res. Lett.*, 28, 3629–3632, 2001.
- Mauldin, R. L., Kosciuch, E., Henry, B., Eisele, F. L., Shetter, R., Lefer, B., Chen, G., Davis, D., Huey, G., and Tanner, D.: Measurements of OH, HO₂ + RO₂, H₂SO₄, and MSA at the south pole during ISCAT 2000, *Atmos. Environ.*, 38, 5423–5437, doi:10.1016/j.atmosenv.2004.06.031, 2004.
- Mauldin, R., Kosciuch, E., Eisele, F., Huey, G., Tanner, D., Sjostedt, S., Blake, D., Chen, G., Crawford, J., and Davis, D.: South Pole Antarctica observations and modeling results: New insights on HO_x radical and sulfur chemistry, *Atmos. Environ.*, 44, 572–581, doi:10.1016/j.atmosenv.2009.07.058, 2010.
- Mayewski, P. A. and Bender, M.: The GISP2 ice core record- paleoclimate highlights, *Rev. Geophys.*, 33, 1287–1296, 1995.
- Neuman, J. A., Nowak, J. B., Huey, L. G., Burkholder, J. B., Dibb, J. E., Holloway, J. S., Liao, J., Peischl, J., Roberts, J. M., Ryerson, T. B., Scheuer, E., Stark, H., Stickel, R. E., Tanner, D. J., and Weinheimer, A.: Bromine measurements in ozone depleted air over the Arctic Ocean, *Atmos. Chem. Phys.*, 10, 6503–6514, doi:10.5194/acp-10-6503-2010, 2010.
- Read, K. A., Mahajan, A. S., Carpenter, L. J., Evans, M. J., Faria, B. V. E., Heard, D. E., Hopkins, J. R., Lee, J. D., Moller, S. J., Lewis, A. C., Mendes, L., McQuaid, J. B., Oetjen, H., Saiz-Lopez, A., Pilling, M. J., and Plane, J. M. C.: Extensive halogen-mediated ozone destruction over the tropical Atlantic Ocean, *Nature*, 453, 1232–1235, doi:10.1038/nature07035, 2008.
- Ren, X. R., Olson, J. R., Crawford, J. H., Brune, W. H., Mao, J. Q., Long, R. B., Chen, Z., Chen, G., Avery, M. A., Sachse, G. W., Barrick, J. D., Diskin, G. S., Huey, L. G., Fried, A., Cohen, R. C., Heikes, B., Wennberg, P. O., Singh, H. B., Blake, D. R., and Shetter, R. E.: HO_x chemistry during INTEX-A 2004: Observation, model calculation, and comparison with previous studies, *J. Geophys. Res.-Atmos.*, 113,

- D05310, doi:10.1029/2007jd009166, 2008.
- Ryerson, T. B., Williams, E. J., and Fehsenfeld, F. C.: An efficient photolysis system for fast-response NO₂ measurements, *J. Geophys. Res.-Atmos.*, 105, 26447–26461, 2000.
- Saiz-Lopez, A., Shillito, J. A., Coe, H., and Plane, J. M. C.: Measurements and modelling of I₂, IO, OIO, BrO and NO₃ in the mid-latitude marine boundary layer, *Atmos. Chem. Phys.*, 6, 1513–1528, doi:10.5194/acp-6-1513-2006, 2006.
- Saiz-Lopez, A., Mahajan, A. S., Salmon, R. A., Bauguutte, S. J. B., Jones, A. E., Roscoe, H. K., and Plane, J. M. C.: Boundary layer halogens in coastal Antarctica, *Science*, 317, 348–351, doi:10.1126/science.1141408, 2007.
- Sander, S. P., Friedl, R. R., Golden, D. M., Kurylo, M. J., Moortgat, Keller-Rudek, H., G. K., Wine, P. H., Ravishankara, A. R., Kolb, C. E., Molina, M. J., Finlayson-Pitts, B., Huie, R. E., and Orkin, V. L.: Chemical Kinetics and Photochemical Data for Use in Atmospheric Studies Evaluation Number 15, JPL Publ. 06-2, NASA Jet Propulsion Laboratory, California Institute of Technology, Pasadena, CA, 2006.
- Shetter, R. E. and Muller, M.: Photolysis frequency measurements using actinic flux spectroradiometry during the PEM-Tropics mission: Instrumentation description and some results, *J. Geophys. Res.-Atmos.*, 104, 5647–5661, 1999.
- Sjostedt, S. J.: Investigation of photochemistry at high latitudes: comparison of model predictions to measurements of short lived species, Ph.D thesis, Georgia Institute of Technology, Atlanta, 2006.
- Sjostedt, S. J., Huey, L. G., Tanner, D. J., Peischl, J., Chen, G., Dibb, J. E., Lefer, B., Hutterli, M. A., Beyersdorf, A. J., Blake, N. J., Blake, D. R., Sueper, D., Ryerson, T., Burkhardt, J., and Stohl, A.: Observations of hydroxyl and the sum of peroxy radicals at Summit, Greenland during summer 2003, *Atmos. Environ.*, 41, 5122–5137, doi:10.1016/j.atmosenv.2006.06.065, 2007.
- Slusher, D. L., Pitteri, S. J., Haman, B. J., Tanner, D. J., and Huey, L. G.: A chemical ionization technique for measurement of pernitric acid in the upper troposphere and the polar boundary layer, *Geophys. Res. Lett.*, 28, 3875–3878, 2001.
- Slusher, D. L., Huey, L. G., Tanner, D. J., Chen, G., Davis, D. D., Buhr, M., Nowak, J. B., Eisele, F. L., Kosciuch, E., Mauldin, R. L., Lefer, B. L., Shetter, R. E., and Dibb, J. E.: Measurements of pernitric acid at the South Pole during ISCAT 2000, *Geophys. Res. Lett.*, 29, 2011, doi:10.1029/2002gl015703, 2002.
- Steffen, A., Douglas, T., Amyot, M., Ariya, P., Aspmo, K., Berg, T., Bottenheim, J., Brooks, S., Cobbett, F., Dastoor, A., Dommergue, A., Ebinghaus, R., Ferrari, C., Gardfeldt, K., Goodsite, M. E., Lean, D., Poulain, A. J., Scherz, C., Skov, H., Sommar, J., and Temme, C.: A synthesis of atmospheric mercury depletion event chemistry in the atmosphere and snow, *Atmos. Chem. Phys.*, 8, 1445–1482, doi:10.5194/acp-8-1445-2008, 2008.
- Streit, G. E.: Negative-ion chemistry and the electron-affinity of SF₆, *J. Chem. Phys.*, 77, 826–833, 1982.
- Stutz, J. and Platt, U.: Improving long-path differential optical absorption spectroscopy with a quartz-fiber mode mixer, *Appl. Optics*, 36, 1105–1115, 1997.
- Stutz, J., Oh, H. J., Whitlow, S. I., Anderson, C., Dibbb, J. E., Flynn, J. H., Rappengluck, B., and Lefer, B.: Simultaneous DOAS and mist-chamber IC measurements of HONO in Houston, TX, *Atmos. Environ.*, 44, 4090–4098, doi:10.1016/j.atmosenv.2009.02.003, 2010.
- Stutz, J., Thomas, J. L., Hurlock, S. C., Schneider, M., von Glasow, R., Piot, M., Gorham, K., Burkhardt, J. F., Ziemba, L., Dibb, J. E., and Lefer, B. L.: Longpath DOAS observations of surface BrO at Summit, Greenland, *Atmos. Chem. Phys. Discuss.*, 11, 6707–6736, doi:10.5194/acpd-11-6707-2011, 2011.
- Swanson, A. L., Blake, N. J., Dibb, J. E., Albert, M. R., Blake, D. R., and Rowland, F. S.: Photochemically induced production of CH₃Br, CH₃I, C₂H₅I, ethene, and propene within surface snow at Summit, Greenland, *Atmos. Environ.*, 36, 2671–2682, 2002.
- Tanner, D. J., Jefferson, A., and Eisele, F. L.: Selected ion chemical ionization mass spectrometric measurement of OH, *J. Geophys. Res.-Atmos.*, 102, 6415–6425, 1997.
- Thomas, J. L., Stutz, J., Lefer, B., Huey, L. G., Toyota, K., Dibb, J. E., and von Glasow, R.: Modeling chemistry in and above snow at Summit, Greenland - Part 1: Model description and results, *Atmos. Chem. Phys.*, 11, 4899–4914, doi:10.5194/acp-11-4899-2011, 2011.
- Tuckermann, M., Ackermann, R., Golz, C., LorenzenSchmidt, H., Senne, T., Stutz, J., Trost, B., Unold, W., and Platt, U.: DOAS-observation of halogen radical-catalysed arctic boundary layer ozone destruction during the ARCTOC-campaigns 1995 and 1996 in Ny-Alesund, Spitsbergen, *Tellus B*, 49, 533–555, 1997.
- Wachsmuth, M., Gäggeler, H. W., von Glasow, R., and Ammann, M.: Accommodation coefficient of HOBr on deliquescent sodium bromide aerosol particles, *Atmos. Chem. Phys.*, 2, 121–131, doi:10.5194/acp-2-121-2002, 2002.
- Yang, J., Honrath, R. E., Peterson, M. C., Dibb, J. E., Sumner, A. L., Shepson, P. B., Frey, M., Jacobi, H. W., Swanson, A., and Blake, N.: Impacts of snowpack emissions on deduced levels of OH and peroxy radicals at Summit, Greenland, *Atmos. Environ.*, 36, 2523–2534, 2002.
- Ziemba, L. D., Dibb, J. E., Griffin, R. J., Huey, L. G., and Beckman, P.: Observations of particle growth at a remote, Arctic site, *Atmos. Environ.*, 44, 1649–1657, doi:10.1016/j.atmosenv.2010.01.032, 2010.